Kuwait J. Sci. **46 (3)** pp. 60-70, 2019

Optoelectronic properties of 3-acetyl-6-bromocoumarin compound in various solvents and concentrations

Adnan Kurt[1*], Bayram Gündüz[2], Zülfiye Ilter[3], Murat Koca[4]

[1]*Dept. of Chemistry, Faculty of Science and Arts, Adiyaman University, Adiyaman/Turkey*
[2]*Dept. of Sciences, Faculty of Education, Muş Alparslan University, Muş/Turkey*
[3]*Dept. of Chemistry, Faculty of Science, Firat University, Elazığ/Turkey*
[4]*Dept. of Pharm. Chemistry, Pharmacy Faculty, Adiyaman University, Adiyaman/Turkey*

**Corresponding author: akurt@adiyaman.edu.tr*

Abstract

In present study, the optoelectronic parameters of a coumarin-derived compound, 3-acetyl-6-bromocoumarin (ABRC), were studied for various solvents and concentrations. The investigated parameters were absorbance band edge, mass extinction coefficient, optical band gap, refractive index, real and imaginary parts of complex dielectric constant, incidence and refraction angle, contrast, optical and electrical conductance. The optical band gap values of 3-acetyl-6-bromocoumarin in DMF and DMSO solvents were found to be 3.110 eV and 3.092 eV at the same concentration of 120 μM, respectively. In addition, the optical band gap decreased from 3.151 to 2.823 eV with increasing concentration from 27 μM to 23 mM. The refractive indices of compound are discussed in detail using Herve-Vandamme, Kumar-Singh, Moss, Ravindra and Reddy methods. A comparative analysis of the results is presented . The results showed that the ABRC material exhibited semiconductor behavior and might be used in optoelectronic devices such as diodes and sensors.

Keywords: Coumarin, optoelectronic properties, optical and electrical conductance, semiconductor, solvent and concentration effect.

1. Introduction

Coumarins constitute one of the major classes of naturally occurring compounds. They are widely isolated from plants and can also be synthesized in laboratories (Ajani & Nwinyi, 2010). In general, coumarins are distinctive compounds due to their chemical structures which render them useful. Coumarins and their derivatives exhibit important photo-physical and spectroscopic properties because they have π-conjugated bonds (Tathe *et al.,* 2015; Tasior *et al.,* 2015). The industrial and technological applications of coumarins increase depending on those properties (Liu *et al.,* 2012). In addition, they allow for different material designs such as organic light-emitting diodes (Swanson *et al.,* 2003), electroluminescence (Zhang *et al.,* 2007), fluorescence materials (Jones & Rahman, 1994), nonlinear optical materials (Gindre *et al.,* 2016), photo-alignment of liquid crystalline molecules (Kim *et al.,* 2006), charge-transfer agents (Donovalova *et al.,* 2012), two-photon absorption materials (Gindre *et al.,* 2013), organic–inorganic hybrid materials (Chen *et al.,* 2015) and laser dyes (Bakhtiari *et al.,* 2014).

As mentioned, the synthesis of these natural or novel synthetic coumarins and their derivatives with various functional groups are possible in the laboratory (Ajani & Nwinyi, 2010). To date, many chemical reactions have been examined that may be utilized to synthesize various coumarin derivatives. One of them is 3-acetyl-6-bromocoumarin (or IUPAC: 3-acetyl-6-bromo-2H-chromen-2-one) compound. In recent years, some studies have been performed to determine different properties related to this compound. For example, Castro *et al.* (2016) carried out a theoretical study on the third-order nonlinear optical properties and structural characterization of the crystal 3-acetyl-6-bromocoumarin They calculated the linear polarizability and the second hyperpolarizability using a new supermolecule approach combined with an iterative electrostatic scheme. They also determined that

the results of calculations of the HOMO and LUMO energies show the occurrence of charge transfer inside the molecule. Ramoji *et al.* (2010) investigated the vibrational studies of 3-acetyl-6-bromocoumarin and 3-acetyl-6-methylcoumarin using infrared absorption and raman spectra. They discovered that the rotation of the acetyl group with respect to the coumarin ring results in one trans conformer being the most stable. In another study, Gupta *et al.* (2011) reported the synthesis and analgesic activity of novel pyrimidine derivatives from 3-acetylcoumarins. Kasumbwe *et al.* (2014) studied the antimicrobial and antioxidant activities of some substituted halogenated coumarins including 3-acetyl-6-bromo-2H-chromen-2-one. Kokila *et al.* (1996) postulated that the crystal structure of 3-acetyl-6-bromocoumarin is planar and makes a dihedral angle of 6.6(4)° with the mean plane of the acetyl group attached to 3-position. Finally, Gomha *et al.* (2015) reported on the utility of 3-acetyl-6-bromo-2H-chromen-2-one for the synthesis of new heterocycles as potential antiproliferative agents.

Some works have been established to define the various properties as is exemplified above. However, no paper has been reported on the optoelectronic parameters of 3-acetyl-6-bromocoumarin in different solvents and concentrations based our current literature knowledge. Owing to the importance of this literature deficiency, here we have described the optoelectronic parameters of 3-acetyl-6-bromocoumarin compound in various solvents and concentrations. These parameters are absorbance, transmittance, absorbance band edge, mass extinction coefficient, optical band gap, refractive index, real and imaginary parts of complex dielectric constant, incidence and refraction angle, contrast, optical and electrical conductance.

2. Methods

2.1 Materials

For this study, 5-Bromo-2-hydroxybenzaldehyde, ethyl acetoacetate and piperidine were purchased from Sigma-Aldrich to act as analytical reagents. All the solvents, acetone, methanol, tetrahydrofuran, N,N-dimethylformamide, dimethyl sulfoxide, diethyl ether, chloroform and ethanol were also obtained from Sigma-Aldrich.

2.2 Instrumental techniques

The infrared characterizations of coumarin compound were performed by using a Perkin Elmer Spectrum 100 FTIR spectrometer with an ATR accessory. A Bruker 300 Mhz Ultrashield TM instrument was used to characterize the compounds by nuclear magnetic resonance (^{1}H-NMR) technique. The optical measurements of the ABRC solutions were recorded with an UV-1800 Spectrophotometer (Shimadzu model) in the wavelength range of 1100-190 nm at room temperature in dark medium. An AND-GR-200 Series Analytical Balance was used to prepare the ABRC solutions.

2.3 Synthesis of 3-acetyl-6-bromocoumarin (ABRC) compound

5-Bromo-2-hydroxybenzaldehyde (5.000 g, 24.87 mmol) and ethyl acetoacetate (3.236 g, 24.87 mmol) were added to a three-necked reaction balloon and dissolved in 50 ml of methanol. After just three drops of piperidine (catalyst) was added drop-wise to the reaction mixture, it was continuously refluxed-stirred on a magnetic stirrer for 24 hours. The reaction mixture was poured into the excessive methanol. The yellowish precipitate of 3-acetyl-6-bromocoumarin (ABRC) was filtered and dried, respectively. The synthesis of ABRC is illustrated in Scheme 1.

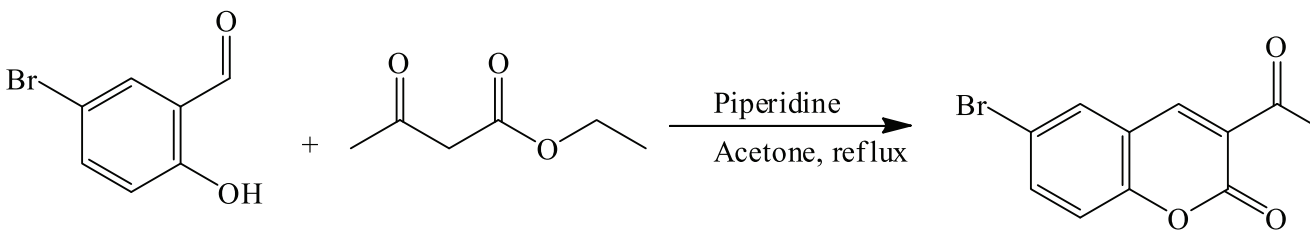

Scheme 1. Synthesis of 3-acetyl-6-bromocoumarin compound

The spectral characterizations were accomplished by FTIR and ^{1}H-NMR techniques as following:

FTIR (cm^{-1}): 3092-3018 and 2989-2880 (aromatic and aliphatic C-H stretching), 1700 (acetyl carbonyl stretching), 1694 (lactone carbonyl stretching), 1621 (lactone C=C stretching) and 1605 (aromatic C=C stretching).

^{1}H-NMR (DMSO, δppm): 8.6 (O-H proton in coumarin ring), 7.7 and 6.7 (aromatic =CH- protons), 6.4 (aliphatic =CH- proton in coumarin ring), 4.9 (–CH_2Cl protons), 3.3 and 2.5 (DMSO solvent).

2.4 Preparation of ABRC solutions

The required amounts of the ABRC compound were dissolved in DMSO and DMF solvents. The ABRC concentrations in these solvents were kept at 120 µM and then the optical measurements for the two solvent systems were performed. Also, to determine the effect of concentration on the optical parameters, the ABRC/ DMSO solutions were prepared at various concentrations of 27 µM, 64 µM, 144 µM, 320 µM and 23 mM (23000 µM) with the solution method.

3. Results and discussion

3.1 Optical properties of ABRC solutions for different solvents

The relation among absorbance, molar extinction coefficient (ε), molar concentration (c) and length (L) of the optical path is given by Beer-Lambert law in Equation 1 (Beer, 1852; Gündüz, 2013):

$$Abs = \varepsilon cL \quad (1)$$

Absorbance (*Abs*) spectra of the ABRC solutions for different solvents at 120 µM are shown in Figure 1. The ABRC compound exhibited a maximum peak at 295 nm corresponding to the near ultraviolet (NUV) region for both DMF and DMSO solvents. The ABRC exhibited another peak at 348 and 349 nm for DMF and DMSO solvents, respectively. These peaks belong to the visible (V) region. The absorbance spectra of the ABRC were not observed at wavelengths of less than about 260 nm. The absorbance values obtained for DMSO were little more than the absorbance values for the DMF solvent.

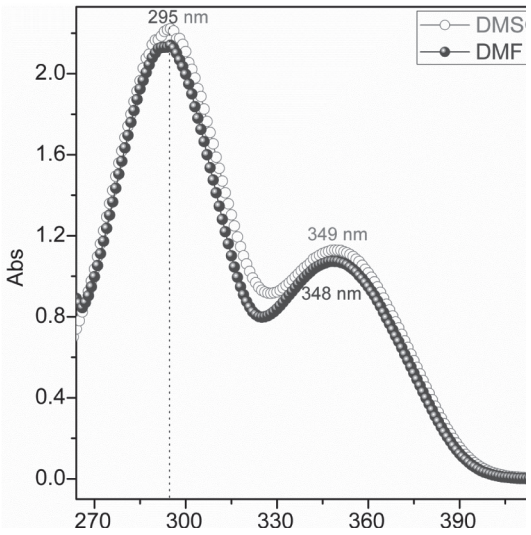

Fig. 1. Absorbance spectra of ABRC solutions for DMF and DMSO solvents

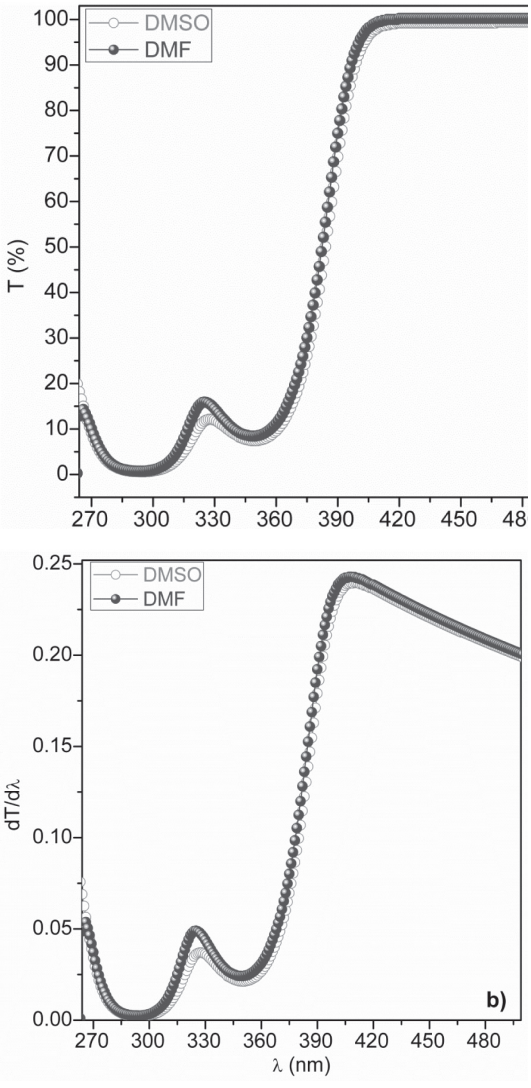

Fig. 2(a). Transmittance spectra and **(b)** the dT/dλ curves vs. wavelength (λ) of ABRC solutions for DMF and DMSO solvents.

Transmittance (*T*) spectra of ABRC solutions for DMF and DMSO solvents are shown in Figure 2(a). The figure shows that the *T* values of the ABRC increased sharply from about 350 to 410 nm, then continued to be constant. We obtained the absorbance band edges ($E_{Abs\text{-}be}$) of the ABRC from the maximum peaks using the dT/dλ in comparison to wavelength (λ) (Figure 2(b)). The $E_{Abs\text{-}be}$ values of the ABRC for DMF and DMSO solvents were found to be 3.047 and 3.024 eV, respectively. These results showed that the absorbance band edge of the ABRC for DMF was higher than the absorbance band edge of the ABRC for DMSO at the same concentration.

The mass extinction coefficient (α_{mass}) depends on the molar extinction coefficient (Orek *et al.,* 2017; Gündüz, 2015) and is given by:

$$\alpha_{mass} = \frac{Abs}{cLM_A}, \quad (2)$$

where M_A is the molecular weight, which is 267,022 g/mol for ABRC. The mass extinction coefficient values of the ABRC solutions for DMF and DMSO solvents were calculated using Equation 2.

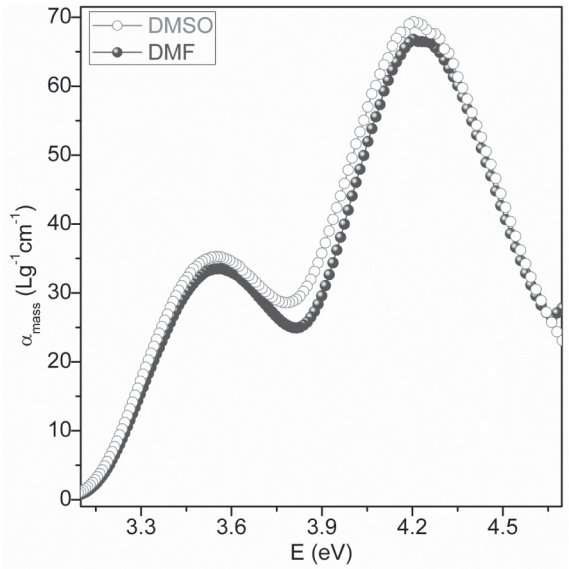

Fig. 3. The mass extinction coefficient (α_{mass}) curves vs. photon energy (*E*) of ABRC solutions for DMF and DMSO solvents.

Figure 3 shows the α_{mass} curves versus photon energy (*E*) of the ABRC for these solvents. The ABRC compound has the maximum peaks at the same photon energy (4.203 eV), whereas the maximum mass extinction coefficients ($\alpha_{max\text{-}mass}$) are different from each other. The $\alpha_{max\text{-}mass}$ value (69,341 Lg^{-1}cm^{-1}) of the ABRC for DMSO was higher than the $\alpha_{max\text{-}mass}$ value (66.786 Lg^{-1}cm^{-1}).

The optical band gap (E_g) is an important optical and optoelectronic parameter and can be estimated from the Tauc model given by Tauc & Menth (1972) as:

$$\alpha(h\vartheta) = A(E - E_g)^n, \quad (3)$$

where α is absorption coefficient, $h\vartheta$ (and *E*) is the photon energy, *A* is a constant and *n* determines the type of optical transitions. For the ABRC compound, *n* was found to be ½ corresponded to allow a direct band gap. For this *n* value, we plotted the $(\alpha h\vartheta)^2$ curves versus *E* of the ABRC solutions for DMF and DMSO solvents (Figure 4).

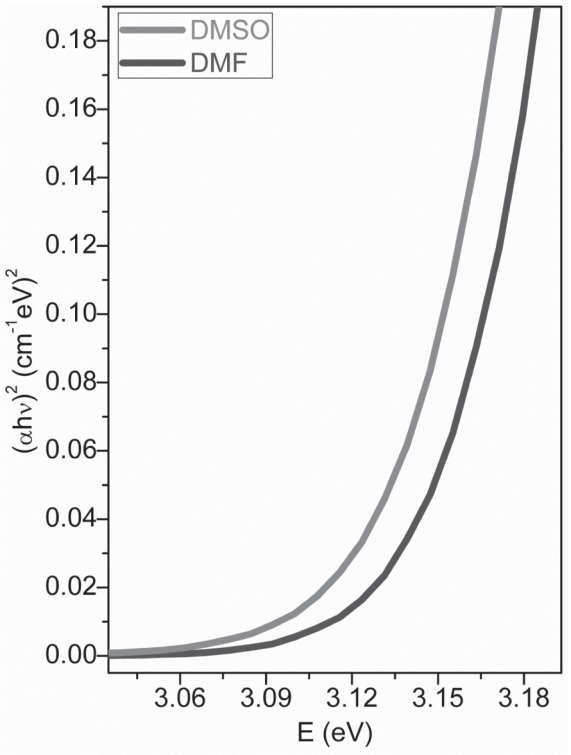

Fig. 4. The $(\alpha h\vartheta)^2$ curves vs. *E* of ABRC solutions for DMF and DMSO solvents.

We obtained the E_g values of the ABRC for DMF and DMSO by extrapolating the linear plot to $(\alpha h\vartheta)^2 = 0$. The optical band gaps of the ABRC for DMF and DMSO at the same concentration of 120 µM were found to be 3.110 eV and 3.092 eV, respectively. These results suggest that the optical band gap for DMSO solvent was lower than that for the DMF solvent, and optical band gap results were consistent with the absorbance band edge results. According to the optical band gaps, the ABRC material exhibited a semiconductor behavior.

The refractive index (*n*) is another significant type of optical and optoelectronic parameter, it can be explained with reflectance (*R*) and is calculated from the following equation (Gündüz, 2015; Abeles, 1972):

$$n = \left\{ \sqrt{\frac{4R}{(R-1)^2} - k^2} - \frac{R+1}{R-1} \right\} \quad (4)$$

where k=αλ/4π. We calculated the *n* values of the ABRC solutions for DMF and DMSO solvents. Figure 5 shows the n curves versus the angular frequency (*ω*). The ABRC exhibited a normal dispersion behavior in related regions, where the refractive indices increased with increasing angular frequency. The refractive index values for the DMSO solvent were also higher than that for DMF.

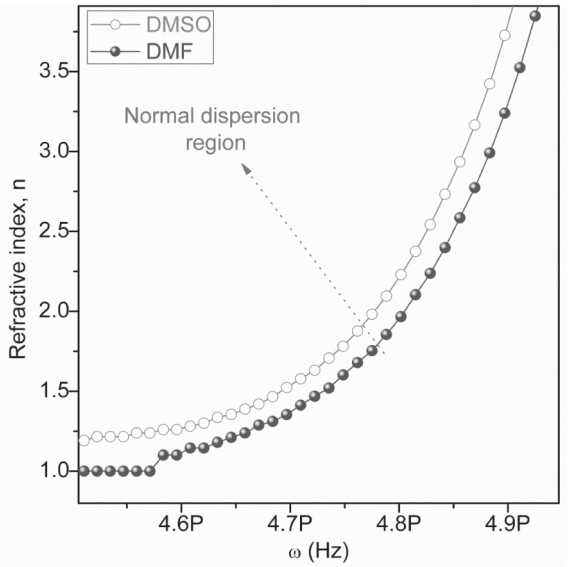

Fig. 5. The refractive index (n) curves vs. angular frequency (ω) of ABRC solutions for DMF and DMSO solvents.

The complex dielectric constant ($\hat{\varepsilon}$) includes the real part (ε_1) and imaginary part (ε_2) as in the following equation:

$$\hat{\varepsilon} = \varepsilon_1 + i\varepsilon_2, \quad (5)$$

where ε_1 and ε_2 parameters are given by:

$$\varepsilon_1 = n^2 - k^2, \quad (6)$$

and

$$\varepsilon_2 = 2nk. \quad (7)$$

The ε_1 and ε_2 parameters were calculated from Equations 6 and 7, respectively. Figure 6 (a,b) indicates the ε_1 and ε_2 curves versus *E* of the ABRC for DMF and DMSO. As seen in this figure, the ABRC shows the maximum peaks of the ε_1 and ε_2 at 4.203 eV for both the DMF and DMSO solvents. The ε_1 values were higher than the ε_2 values.

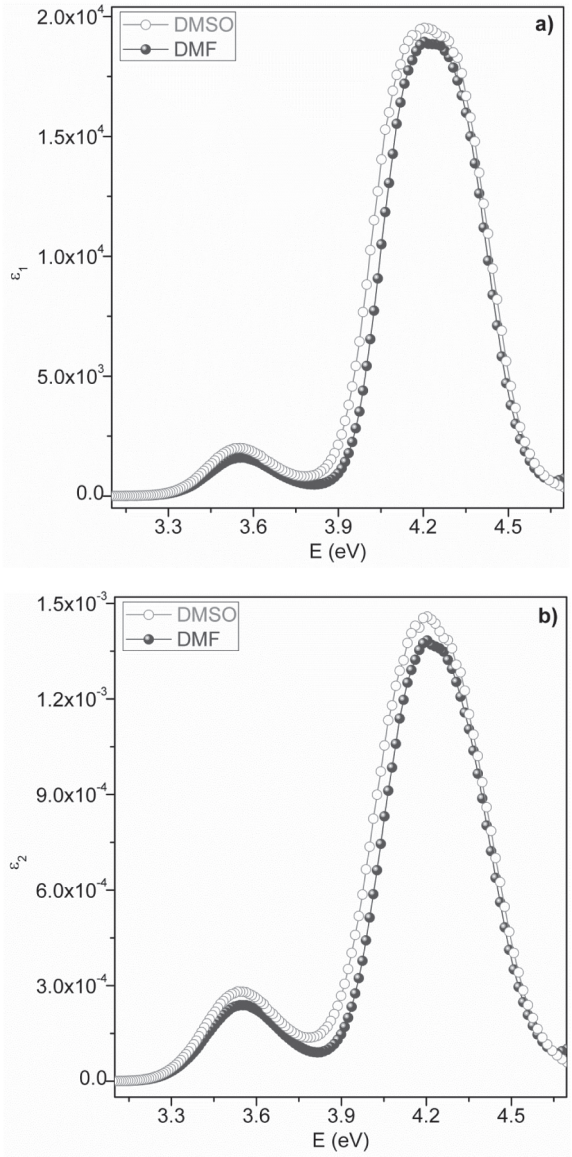

Fig. 6. The **(a)** real part (ε_1) and **(b)** imaginary part (ε_2) curves of the complex dielectric constant vs. E of ABRC solutions for DMF and DMSO solvents.

The incidence angle (Φ_1) and refraction angle (Φ_2) play an operational role in optical and optoelectronic devices. We calculated the Φ_1 values using the following equation:

$$\Phi_1 = tan^{-1}\left(\frac{n_2}{n_1}\right). \quad (8)$$

Figure 7 shows the Φ_1 plots in comparison to *E* of the ABRC for the DMF and DMSO solvents. The incidence angle values for both solvents were close to each other. We also calculated the Φ_2 values from Equation 9,

$$\Phi_2 = sin^{-1}\left(\frac{n_1}{n_2}\sin\Phi_1\right). \quad (9)$$

Figure 7 also shows the Φ_2 plots versus *E* of the ABRC

for DMF and DMSO solvents. As seen in Figure 7, the incidence angles were higher than the refraction angles.

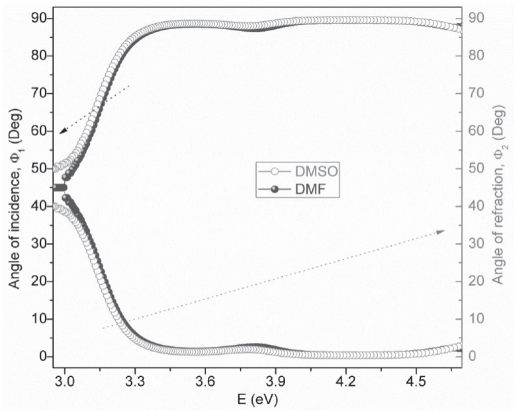

Fig. 7. The incidence angle (Φ_1) and refraction angle (Φ_2) curves vs. E of ABRC solutions for DMF and DMSO solvents.

Sensitivity is an important sensing parameter for optoelectronic devices and depends on contrast (α_c) (Gündüz, 2015). The α_c is given by:

$$\alpha_c = 1 - \left(\frac{n_1}{n_2}\right)^2 \quad (10)$$

The contrast values of the ABRC for DMF and DMSO were calculated from Equation 10. Figure 8 shows their α_c curves in comparison to E. The contrast values of the ABRC increase sharply at about 2.96 to 3.25 eV for both solvents. The ABRC exhibited the sensing properties, which means that it might be used for sensor applications.

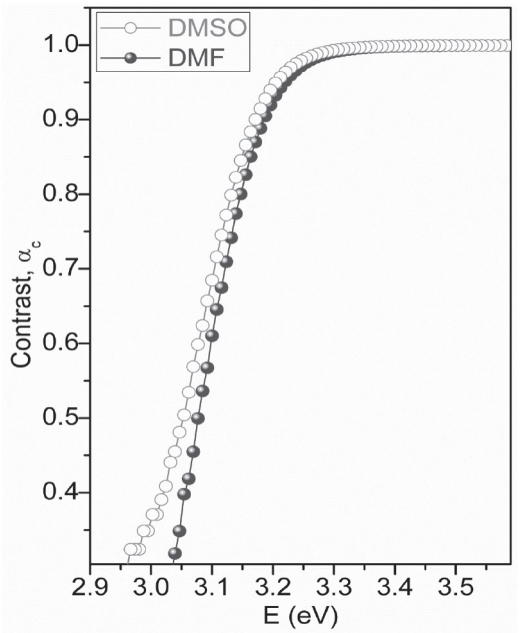

Fig. 8. The contrast (α_c) curves vs. E of ABRC solutions for DMF and DMSO solvents.

Finally, we investigated optical conductance (σ_{opt}) and electrical conductance (σ_{elect}) properties, which play significant roles in optoelectronic applications. The σ_{opt} and σ_{elect} can be explained by Abd El-Raheem (2007):

$$\sigma_{opt} = \frac{\alpha nc}{4\pi}, \quad (11)$$

where c is the velocity of light. σ_{elect} is given as:

$$\sigma_{elect} = \frac{2\lambda\sigma_{opt}}{\alpha} \quad (12)$$

We calculated the σ_{opt} and σ_{elect} values of the ABRC for the DMF and DMSO solvents. Figure 9 (a,b) gives the σ_{opt} and σ_{elect} curves versus E. ABRC had the maximum peaks at 4.203 eV for both solvents, and the σ_{opt} values were about 4x10^8 times bigger than the σ_{elect} values.

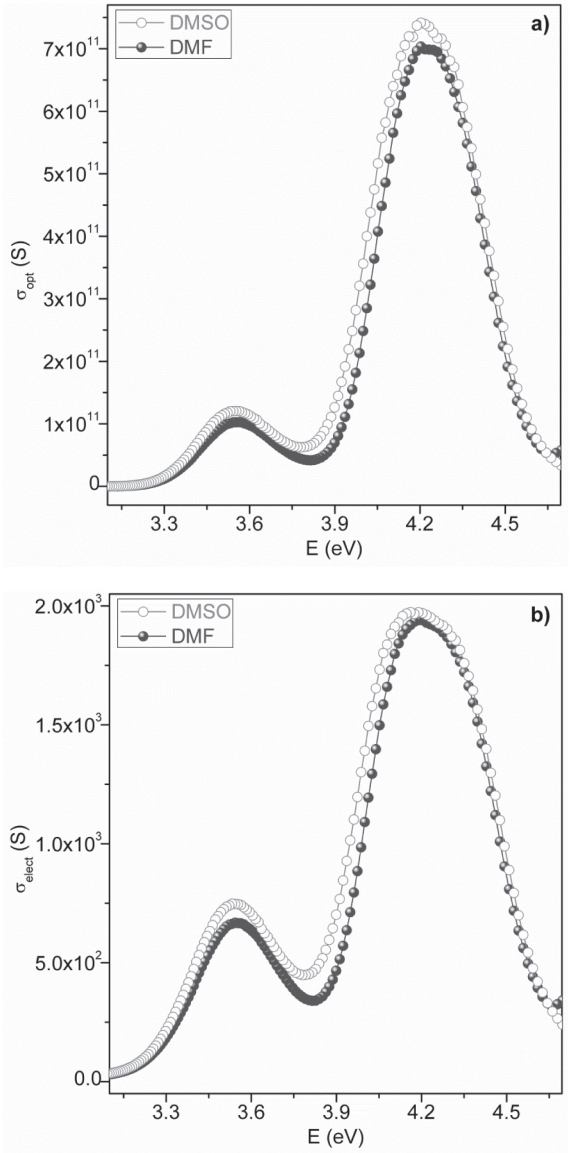

Fig. 9. The **(a)** optical conductance (σ_{opt}) and **(b)** electrical conductance (σ_{elect}) curves vs. E of ABRC solutions for DMF and DMSO solvents.

Table 1. The absorbance band edges ($E_{Abs\text{-}be}$), optical band gap (E_g) and refractive index (n) values obtained from various relations of ABRC solutions for different concentrations

Concentration	$E_{Abs\text{-}be}$ (eV)	E_g (eV)	Refractive indices (*n*)					
			Moss	Ravindra	Herve-Vandamme	Reddy	Kumar-Singh	Average *n*
27 µM	3.092	3.151	2.343	2.131	2.285	2.727	2.326	2.362
64 µM	3.069	3.109	2.351	2.156	2.296	2.737	2.336	2.375
144 µM	3.024	3.070	2.359	2.181	2.308	2.747	2.345	2.388
320 µM	3.002	3.041	2.364	2.199	2.316	2.754	2.353	2.397
23 mM	2.713	2.823	2.409	2.334	2.381	2.813	2.410	2.469

3.2 Optical properties of ABRC solutions for different concentrations.

Absorbance spectra of the ABRC/DMSO solutions for different concentrations (27, 64, 144, 320 µM and 23 mM) were obtained. The absorbance of the ABRC dominated the NUV region, and none of the absorbance spectra was observed for concentrations higher than 144 µM. These results suggested that absorbance increased with increasing concentration.

Transmittance spectra of the ABRC solutions for 27, 64, 144, 320 µM and 23 mM are shown in Figure 10(a). The transmittance values of the ABRC dominated the visible region and decreased with increasing concentration. The $E_{Abs\text{-}be}$ values of the ABRC for 27, 64, 144, 320 µM and 23 mM were obtained from the maximum peaks of the dT/dλ curves in comparison to λ (Figure 10(b) and Table 1). As seen in Table 1, the absorbance band edge of the ABRC decreased from 3.092 to 2.713 eV with increasing concentration.

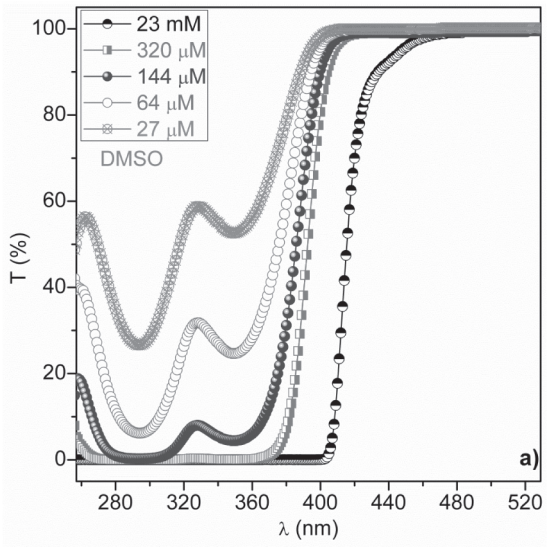

Fig. 10(a). Transmittance spectra of ABRC solutions for 27, 64, 144, 320 µM and 23 mM.

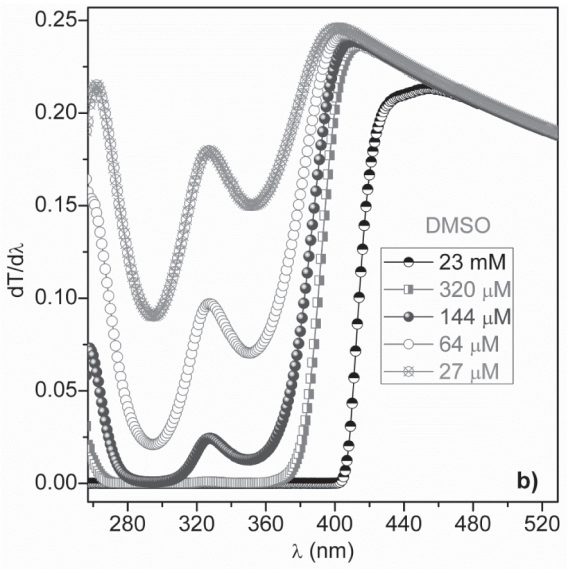

Fig. 10(b). The dT/dλ curves vs. λ of ABRC solutions for 27, 64, 144, 320 µM and 23 mM

To obtain the allowed direct optical band gap of the ABRC solutions for 27, 64, 144, 320 µM and 23 mM, we plotted the $(\alpha h\vartheta)^2$ against the *E*, as seen in Figure 11. We obtained the E_g values of the ABRC for 27, 64, 144, 320 µM and 23 mM by extrapolating the linear plot to $(\alpha h\vartheta)^2 = 0$. The obtained E_g values of the ABRC for 27, 64, 144, 320 µM and 23 mM are given in Table 1. The table shows that the optical band gap of the ABRC decreased from 3.151 to 2.823 eV with increasing concentration.

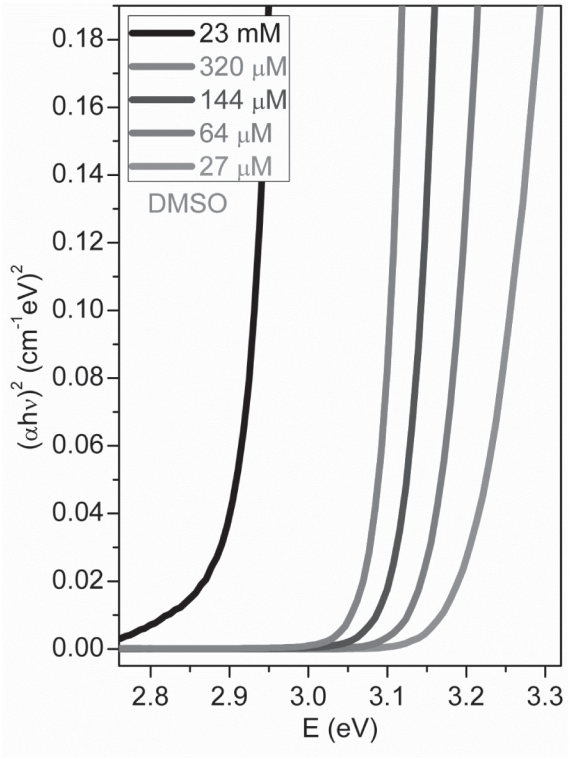

Fig. 11. The $(\alpha h\vartheta)^2$ vs. *E* of ABRC solutions for 27, 64, 144, 320 μM and 23 mM.

We calculated the refractive index values of the ABRC solutions for 27, 64, 144, 320 μM and 23 mM using Equation 4. The *n* curves in comparison to ω of the ABRC were also plotted (Figure 12(a)). The ABRC showed a normal dispersion behavior.

Many relations, such as Herve-Vandamme, Kumar-Singh, Moss, Ravindra and Reddy (Tripathy, 2015; Cabuk & Gündüz, 2017), can be obtained for the refractive index based on optical band gaps. The refractive indices of the ABRC solutions for 27, 64, 144, 320 μM and 23 mM were obtained for the aforementioned relations. Figure 12(b) indicates the n curves versus the concentrations of the ABRC for Herve-Vandamme, Kumar-Singh, Moss, Ravindra and Reddy relations. In addition, to compare these relations, we calculated their refractive index averages (n_{avg}) from Figure 12(b). The *n* values obtained from the Reddy relation were higher than the n_{avg} values, whereas the other values were lower.

The contrast values of the ABRC solutions for 27, 64, 144, 320 μM and 23 mM were calculated from Equation 10 and their α_c curves versus E are shown in Figure 13. The contrast values of the ABRC increased sharply at about 2.65 to 3.37 eV for all concentrations. These results suggest that the contrast of the ABRC might be changed with different concentrations.

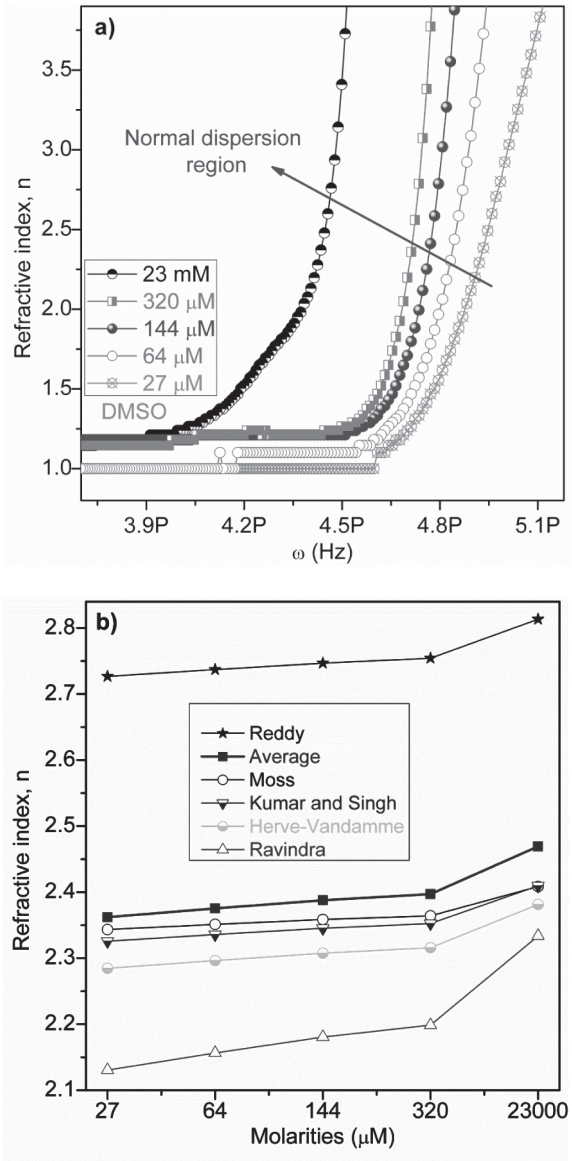

Fig. 12. The **a)** *n* curves vs. ω for 27, 64, 144, 320 μM and 23 mM and **b)** n curves vs. concentrations for Herve-Vandamme, Kumar-Singh, Moss, Ravindra and Reddy relations of the ABRC solutions.

4. Conclusions

3-Acetyl-6-bromocoumarin compound exhibits a maximum absorbance peak at 295 nm corresponding to the near ultraviolet (NUV) region. There was also another peak at 348 nm for the visible (V) region. Not all of the absorbance spectra were observed for concentrations higher than 144 μM. The optical band gap values for DMSO and DMF solvents were found to be 3.110 eV and 3.09 eV, respectively. The absorbance band edge varied from 3.092 eV to 2.713 eV with increasing concentration. The refractive index values obtained from the Reddy relation were higher than the average refractive index values. The optical results obtained in this study show

that 3-acetyl-6-bromocoumarin displays a semiconductor behavior, so it might be an important candidate for many optoelectronic devices, such as diodes, photo-diodes and sensor, etc.

References

Aazam, E.S., El Husseiny, A.F. & Al-Amri, H.M. (2012). Synthesis and photoluminescent properties of a Schiff-base ligand and its mononuclear Zn (II), Cd (II), Cu (II), Ni(II) and Pd (II) metal complexes. Arabian Journal of Chemistry, **5:** 45–53.

Abd El-Raheem, M.M. (2007). Optical properties of GeSeTl thin films. Journal of Physics: Condensed Matter, **19:** 216209–216215.

Abeles, F. (1972). Optical properties of solids. North-Holland Publishing Company, London, Amsterdam.

Ajani, O.O. & Nwinyi, O.C. (2010). Microwave-assisted synthesis and evaluation of antimicrobial activity of 3-{3-(s-aryl and s-heteroaromatic)acryloyl}-2H-chromen-2-one derivatives. Journal of Heterocyclic Chemistry, **47:** 179-187.

Bai, Y. Du, J. & Weng, X. (2014). Synthesis, characterization, optical properties and theoretical calculations of 6-fluoro coumarin, Spectrochimica Acta Part A: Molecular and Biomolecular Spectroscopy, **126:** 14–20.

Bakhtiari, G., Moradi, S. & Soltanali, S. (2014). A novel method for the synthesis of coumarin laser dyes derived from 3-(1H-benzoimidazol-2-yl) coumarin-2-one under microwave irradiation, Arabian Journal of Chemistry, **7:** 972–975.

Beer, A. (1852) Determination of the absorption of red light in colored liquids, Annalen der Physik und Chemie, **86:** 78–88.

Cabuk, M. & Gündüz, B. (2017). Controlling the optical properties of polyaniline doped by boric acid particles by changing their doping agent and initiator concentration. Applied Surface Science, **424:** 345–351.

Castro, A.N., Almeida, L.R., Anjos, M.M., Oliveira, G.R., Napolitano, H.B., Valverde, C. & Baseia, B. (2016). Theoretical study on the third-order nonlinear optical properties and structural characterization of 3-acetyl-6-bromocoumarin. Chemical Physics Letters, **653:** 122–130.

Chen, W., Tong, U.S., Zeng, T., Streb, C. & Song, Y.F. (2015). Reversible photodimerization of coumarin-modified Wells–Dawson anions. Journal of Materials Chemistry C, **3:** 4388-4393.

Donovalova, J., Cigan, M., Stankovicova, H., Gaspar, J., Danko, M., Gaplovsky, A. & Hrdlovic, P. (2012). Spectral properties of substituted coumarins in solution and polymer matrices. Molecules, **17:** 3259-3276.

Gindre, D., Iliopoulos, K., Krupka, O., Champigny, E., Morille, Y. & Sallé, M. (2013). Image storage in coumarin-based copolymer thin films by photoinduced dimerization. Optics Letters, **38:** 4636-4639.

Gindre, D., Iliopoulos, K., Krupka, O., Evrard, M., Champigny, E. & Sallé, M. (2016). Coumarin-Containing polymers for high density non-linear optical data storage. Molecules, **21:** 147.

Gomha, S.M., Zaki, Y.H. & Abdelhamid, A.O. (2015). Utility of 3-Acetyl-6-bromo-2H-chromen-2-one for the synthesis of new heterocycles as potential antiproliferative agents. Molecules, **20:** 21826–21839.

Gupta, J.K., Sharma, P.K., Dudhe, R., Mondal, S.C., Chaudhary, A. & Verma, P.K. (2011). Synthesis and analgesic activity of novel pyrimidine derivatives of coumarin moiety. Acta Poloniae Pharmaceutica - Drug Research, **68:** 785 – 793.

Gündüz, B. (2013). Effects of molarity and solvents on the optical properties of the solutions of tris[4-(5-dicyanomethylidenemethyl-2-thienyl) phenyl] amine (TDCV-TPA) and structural properties of its film. Optical Materials, **36:** 425-436.

Gündüz, B. (2015). Optical properties of poly[2-methoxy-5-(3′,7′-dimethyloctyloxy)-1,4-phenylenevinylene] light-emitting polymer solutions: Effects of molarities and solvents, Polymer Bulletin, **72:** 3241-3267.

Jones, G. & Rahman, M.A. (1994). Fluorescence properties of coumarin laser dyes in aqueous polymer media. chromophore ısolation in poly(methacrylic acid) hypercoils, Journal of Physical Chemistry, **98:** 13028–13037

Kasumbwe, K., Venugopala, K.N., Mohanlall, V. & Odhav, B. (2014). Antimicrobial and antioxidant activities of substituted halogenated coumarins. Journal of Medicinal Plant Research, **8:** 274-281.

Kim, C., Trajkovska, A., Wallace, J.U. & Chen, S.H. (2006). New insight into photoalignment of liquid crystals on coumarin-containing polymer films. Macromolecules, **39:** 3817-3823.

Kokila, M.K., Puttaraja, Kulkarni, M.V. & Shivaprakash, N.C. (1996). 3-Acetyl-6-bromocoumarin, Acta Crystallographica Section C, **52:** 2078-2081.

Liu, X., Cole, J.M., Waddell, P.G., Lin, T.C., Radia, J. & Zeidler, A. (2012). Molecular origins of optoelectronic properties in coumarin dyes: Toward designer solar cell and laser applications. Journal of Physical Chemistry A, **116:** 727–737.

Liu, X., Xu, Z. & Cole, J.M. (2013). Molecular design of uv–vis absorption and emission properties in organic fluorophores: Toward larger bathochromic shifts, enhanced molar extinction coefficients, and greater stokes shifts. The Journal of Physical Chemistry C, **117:** 16584-16595.

Orek, C., Gündüz, B., Kaygili, O. & Bulut, N. (2017). Electronic, optical, and spectroscopic analysis of TBADN organic semiconductor: Experiment and theory. Chemical Physics Letters, **678:** 130–138.

Pajk, S. (2014). Synthesis and fluorescence properties of environment-sensitive 7-(diethylamino)coumarin derivatives. Tetrahedron Letters, **55:** 6044–6047.

Rabahi, A., Makhloufi-Chebli, M., Hamdi, S.M., Silva, A.M.S., Kheffache, D., Kheddis, B.B. & Hamdi, M. (2014). Synthesis and optical properties of coumarins and iminocoumarins: Estimation of ground- and excited-state dipole moments from a solvatochromic shift and theoretical methods. Journal of Molecular Liquids, **195:** 240-247.

Ramoji, A., Yenagi, J., Tonannavar, J., Jadhav, V.B. & Kulkarni, M.V. (2010). Vibrational and ab initio studies of 3-acetyl-6-bromocoumarin and 3-acetyl-6-methylcoumarin. Spectrochimica Acta Part A, **77:** 1039–1047.

Sinha, S., Kumaran, A.P., Mishra, D. & Paira, P. (2016). Synthesis and cytotoxicity study of novel 3-(triazolyl) coumarins based fluorescent scaffolds. Bioorganic & Medicinal Chemistry Letters, **26:** 5557–5561.

Swanson, S.A., Wallraff, G.M., Chen, J.P., Zhang, W.J., Bozano, L.D., Carter, K.R., Salem, J.R., Villa, R. & Scott, J.C. (2003). Stable and efficient fluorescent red and green dyes for external and internal conversion of blue OLED emission. Chemistry of Materials, **15:** 2305-2312.

Tasior, M., Kim, D., Singha, S., Krzeszewski, M., Ahn, K.H. & Gryko, D.T. (2015). π-Expanded coumarins: synthesis, optical properties and applications. Journal of Materials Chemistry C, **3:** 1421-1446.

Tathe, A.B., Gupta, V.D. & Sekar, N. (2015). Synthesis and combined experimental and computational investigations on spectroscopic and photophysical properties of red emitting 3-styryl coumarins. Dyes and Pigments, **119:** 49–55.

Tauc, J. & Menth, A. (1972). States in the gap. Journal of Non-Crystalline Solids, **8–10:** 569–585.

Tripathy, S.K. (2015). Refractive indices of semiconductors from energy gaps. Optical Materials, **46:** 240-246.

Zhang, H., Yu, T., Zhao, Y., Fan, D., Qian, L., Yang, C. & Zhang, K. (2007). Syntheses, characterization and fluorescent properties of two triethylene-glycol dicoumarin-3-carboxylates. Spectrochimica Acta Part A: Molecular and Biomolecular Spectroscopy, **68:** 725–727.

Submitted: 05/02/2018
Revised: 12/12/2018
Accepted: 16/01/2019

الخواص الإلكتروضوئية لمركب 3 – أسيتيل – 6 – بروموكومارين في مختلف المذيبات والتركيزات

[1,*] عدنان كورت ، [2] بيرم غندوز ، [3] زولفيي إلتر ، [4] مراد كوكا

[1] قسم الكيمياء، كلية العلوم والآداب، جامعة أديامان، أديامان، تركيا
[2] قسم العلوم، كلية التربية، جامعة موس البارسلان، تركيا
[3] قسم الكيمياء، كلية العلوم، جامعة فرات، إيلازي، تركيا
[4] قسم الصيدلة الكيميائية، كلية الصيدلة، جامعة أديامان، أديامان، تركيا

[*] المؤلف: *akurt@adiyaman.edu.tr*

الملخص

في هذه الدراسة، تمت دراسة المعلمات الإلكترونية الضوئية لمركب مشتق من الكومارين، 3 –أسيتيل– 6 – بروموكومارين (ABRC)، في مختلف المذيبات والتركيزات. المعلمات التي تمت دراستها، هي: حافة شريط الامتصاص، معامل الانطفاء الكتلي، فجوة النطاق الموجي الضوئي، معامل الانكسار، أجزاء حقيقية وخيالية لثابت العزل الكهربائي المعقد، زاوية السقوط والانكسار، التباين، والمواصلة الضوئية والكهربائية. تم العثور على قيم فجوة النطاق البصري لـ 3 –أسيتيل– 6 –بروموكومارين في مذيبات DMF و DMSO لتكون 3.110 الكترون فولت و3.092 الكترون فولت بنفس التركيز 120 ميكرومتر، على التوالي. بالإضافة إلى ذلك، انخفضت فجوة النطاق البصري من 3.151 إلى 2.823 الكترون فولت مع زيادة التركيز من 27 ميكرومتر إلى 23 ملم. ونوقشت المؤشرات الانكسارية للمركب بالتفصيل باستخدام طرق هيرفي–فاندامي، كومار سينغ، موس، رافيندرا وريدي. وتمت مقارنة جميع النتائج التي تم الحصول عليها مع بعضها البعض. وأظهرت النتائج أن مادة ABRC قد أبدت سلوك أشباه الموصلات ويمكن أن تُستخدم في الأجهزة الإلكترونية الضوئية مثل الصمام الثنائي وأجهزة الاستشعار.